Cationic and anionic environments in LiTFSI-doped di-ureasils with application in solid-state electrochromic devices

S.C. Nunes [a], V. de Zea Bermudez [a,*], D. Ostrovskii [b], P.C. Barbosa [c], M.M. Silva [c], M.J. Smith [c]

[a] *Departamento de Química and CQ-VR, Universidade de Trás-os-Montes e Alto Douro 5001-801 Vila Real, Portugal*
[b] *Department of Applied Physics, Chalmers University of Technology, 41296 Göteborg, Sweden*
[c] *Departamento de Química, Universidade do Minho, Gualtar, 4710-057 Braga, Portugal*

Received 26 July 2007; accepted 21 January 2008

Abstract

Fourier Transform mid-infrared and Raman spectroscopies were used to investigate the cation/polymer, cation/urea bridge, cation/anion and hydrogen bonding interactions in poly(oxyethylene) (POE)/siloxane di-ureasil networks prepared by the sol–gel route and doped with lithium bis(trifluoromethanesulfonyl)imide (LiTFSI). Materials with compositions $200 \geqslant n \geqslant 5$ (where n expresses the molar ratio OCH_2CH_2/Li^+) were studied. The Li^+ ions coordinate to the urea carbonyl oxygen atoms over the whole range of salt concentration considered. Bonding to the ether oxygen atoms of the POE chains occurs at $n \leqslant 40$, although a significant fraction of the POE chains remains non-coordinated. In these high salt content samples, the cations interact with the anions forming contact ion pairs. "Free" ions are probably the main charge carriers at the room temperature conductivity maximum of these ormolytes.

Keywords: Di-ureasils; LiTFSI; Sol–gel; FT-IR; FT-Raman spectroscopy

1. Introduction

During the last two decades solid polymer electrolytes (SPE) [1] have attracted the attention of many researchers owing to the potential technological impact of these materials in solid-state electrochemistry.

Lithium bis(trifluoromethanesulfone)imide ($LiN(SO_2CF_3)_2$, LiTFSI)-based SPE systems [2–6] generally show higher conductivities than other lithium salts [7] in these electrolyte systems. The observed improvement in ionic conductivity has been attributed to the low lattice energy of the salt, which facilitates the solvation of the lithium salt by the polymer, and to the deslocalized negative charge on the nitrogen and four oxygens atoms, which reduces the tendency to form ion pairs. In addition, because of its shape and internal flexibility, the $TFSI^-$ anion exerts a plasticizing effect and reduces the crystallinity of the SPE, therefore lowering the glass transition temperature of the materials.

This paper is devoted to the study of a family of sol–gel [8] derived POE/siloxane hybrid electrolyte materials, designated as *di-ureasils* [9,10], containing a wide range of LiTFSI concentration. The di-ureasil matrix is a hybrid structure in which the siliceous framework is bonded through urea bridges to POE chains with about 40 oxyethylene repeat units. The LiTFSI-doped di-ureasil samples were represented by the notation d-U(2000)$_n$LiTFSI, where d-U represents the urea bridges at the extremes of the POE chains, 2000 corresponds to the average molecular weight of the organic segment precursor and n indicates the salt composition as molar ratio of OCH_2CH_2 units per cation. Studies carried out very recently [11] allowed us to conclude that the d-U(2000)$_n$LiTFSI ormolytes (organically modified silica electrolytes) have potential applications in optical devices such as rear-view windows and "smart windows". They exhibit a wide electrochemical stability window of over 5.0 V. Given that in solution the urea molecule is known to undergo anodic oxidation [12,13], the stability observed may initially seem anomalous. In previous studies however, interference of urea on biosensor function has been efficiently blocked by the use of a polymeric layer on the biosensing electrode surface [14]. Stability of a urea linkage group incorporated within a polymer electrolyte network has already been reported in POE/siloxane ormolytes [15,16] and it is likely that this stability arises from an encapsulation/protection effect of the chemical environment of the urea linkage. Spectroscopic data confirmed that at low-to-moderate salt content the ionic guest species coordinate with the carbonyl oxygen atoms of the urea linkages and this may also contribute to the observed electrochemical stability. In addition, the d-U(2000)$_n$LiTFSI materials yield higher conductivities than the lithium triflate [15] and lithium perchlorate-based [16] di-ureasil analogues.

In the present paper, we have studied the local chemical environment of the Li^+ and $TFSI^-$ ions in the d-U(2000) medium with the primary objective of gaining insight into the ionic conductivity mechanism. We note that in the d-U(2000)$_n$LiTFSI ormolytes three coordinating sites are available for the cations. Coordination may occur at the urea carbonyl oxygen atoms (–C=O) and at the polymer ether oxygen atoms (–COC–) provided by the host hybrid framework and at the imide ions of the guest salt. The charge carriers in these type of systems may be [7,15–18]: (a) "free" or weakly coordinated ions with high mobility; (b) cations bonded strongly to the host polymer and/or to the urea cross-links with low mobility; (c) ionic aggregates with low-to-moderate mobility.

2. Experimental section

2.1. Materials

Lithium bis(trifluoromethanesulfonyl)imide ($LiN(SO_2CF_3)_2$) was dried under vacuum at 190 °C for 7 days and then stored in a high integrity, dry argon-filled glovebox. The diamine *O*,*O*′-bis(2-aminopropyl) polypropylene glycol-*block*-polyethylene glycol-*block*-polypropylene gly-

* Corresponding author. Tel.: +351 259 350253; fax: +351 259 350480
E-mail address: vbermude@utad.pt (V. de Zea Bermudez).

col (commercially available as Jeffamine ED-2001®, Fluka, average molecular weight 2001 g mol^{-1}) was dried under vacuum at 25 °C for several days prior to use. The bridging agent, 3-isocyanatepropyltriethoxysilane (ICPTES, Aldrich 95%), was used as received. Ethanol (CH_3CH_2OH, Merck, 99.8%) and tetrahydrofuran (THF, Merck, 99.9%) were dried over molecular sieves. High purity distilled water was used in all experiments.

2.2. Preparation of the di-ureasil ormolytes

The preliminary stage of the synthesis of the di-ureasils involved the formation of a covalent bond between the terminal NH_2 groups of Jeffamine-2001® ($a + c = 2.5$ and $b = 40.5$) and the –N=C=O group of ICPTES in THF to yield the urea cross-linked organic–inorganic hybrid precursor designated as di-ureapropyltriethoxysilane (d-UPTES(2000)) (molar ratio Jeffamine 2001®: ICPTES = 1:2) (Scheme 1). The grafting process was infrared monitored. In the second stage of the synthetic procedure, a mixture of CH_3CH_2OH and water was added to the d-UPTES(2000) solution (molar ratio ICPTES:CH_3CH_2-OH:H_2O = 1:4:1.5), followed by the incorporation of $LiN(SO_2CF_3)_2$. Samples with $n = \infty$, 200, 100, 80, 60, 35, 25, 10, 8 and 5 were prepared. The materials were produced as transparent monoliths with a yellowish hue.

2.3. Experimental techniques

2.3.1. Fourier transform infrared (FT-IR) spectroscopy

FT-IR spectra were acquired at room temperature on a Unicam FT-IR spectrophotometer. The spectra were collected over the 4000–400 cm^{-1} range by averaging 120 scans at a wavenumber resolution of 4 cm^{-1}. Solid samples (2 mg) were finely ground, mixed with approximately 175 mg of dried potassium bromide (KBr, Merck, spectroscopic grade) and pressed into pellets.

2.3.2. FT-Raman Spectroscopy

The FT-Raman spectra were recorded with a resolution of 2 cm^{-1} at room temperature with a Bruker IFS-66 spectrometer equipped with a FRA-106 Raman module and a near-infrared continuous YAG laser with wavelength 1064 nm. During the measurements the sample cell was located in an evacuated thermostat and the temperature stability in the sample was estimated to be about 0.3 °C. The spectra were collected over the 3200–300 cm^{-1} range at a resolution of 2 cm^{-1}. The accumulation time for each spectrum was 4 h.

To evaluate complex FT-IR and FT-Raman band envelopes and to identify underlying spectral components, the iterative least-squares curve-fitting procedure in the PeakFit[1] software was used throughout this study. The best fit of the experimental data was obtained by varying the frequency, bandwidth and intensity of the bands and by using Gaussian (FT-IR spectra) and Voight shapes (FT-Raman spectra). A linear baseline correction with a tolerance of 0.2% was employed. The standard errors of the curve-fitting procedure were less than 0.003.

3. Results and discussion

In an attempt to correlate the ionic conductivity data with the extent of ionic association we have examined diagnostic bands of polymer chains, of urea bridges and of the anion which suffer characteristic changes of intensity and/or frequency upon cation coordination.

The fundamental vibrations of the $TFSI^-$ anion are situated below 1400 cm^{-1} [19] If the anion adopts C_2 symmetry, its 39 internal vibrations can be classified into 20 A and 19 B modes, the former being polarized in Raman [19]. In addition, for C_2 symmetry, each of these modes will split into in-phase (A) and out-of-phase (B) components because of the coupling between the two SO_2 groups [19].

3.1. Li^+/polymer interactions

Fig. 1a shows the FT-IR spectra of selected Li^+-doped di-ureasils in the 1210–1040 cm^{-1} interval. The curve-fitting results of the spectra of representative samples in this range of wavenumbers are shown in Fig. 1b. The frequency of the isolated components of this region and their assignment are listed in Table 1.

The characterization of the spectral region where the stretching vibration modes of the polyether skeleton (νCOC) appear (1170–1040 cm^{-1}) is of interest because it is highly sensitive to alterations in the POE conformations arising from interactions between the ether oxygen atoms and the cations.

The νCOC region of the d-U(2000)$_n$LiTFSI samples with $n \geqslant 200$ displays a prominent, broad band centred around 1108 cm^{-1} and a shoulder at about 1146 cm^{-1} (Fig. 1b and Table 1). These features, ascribed to the νCOC vibration mode and to the coupled vibration of the νCOC and rCH$_2$ modes, respectively, are associated with non-coordinated, disordered POE chains [20–22]. The νCOC event at 1108 cm^{-1} typically shifts to lower wavenumbers as a result of the alteration in the chemical environment of the polymer ether oxygen atoms caused by coordination to the cations. The magnitude of the shift depends on the strength of the cation/POE interaction. This effect is clearly detected in the FT-IR spectra of the samples with $n \leqslant 40$, where three new events develop: a band centred at 1194 cm^{-1} and two shoulders at *ca.* 1137 and 1061 cm^{-1} (Fig. 1a). In this range of salt concentration the νCOC band profile was resolved into bands at 1146, 1137, 1108, 1082 and 1060 cm^{-1} (Fig. 1b and Table 1). The band at 1082 cm^{-1} is indicative of the complexation of the cation by the polymer segments [23]. As the strong 1108 cm^{-1} feature persists in the FT-IR spectra of all the samples examined (Fig. 1b), we are led to conclude that a significant proportion of POE chains remains non-complexed. The 1194 and 1137 cm^{-1} components, characteristic of the "free" imide ion, are attributed to the asymmetric stretching mode of the CF_3 group (ν_aCF_3) and to the symmetric out-of-phase stretching mode of the SO_2 group ($\nu_s^{o.p.}SO_2$), respectively [19,24]. The event at 1060 cm^{-1} is also ascribed to an imide band [19,24].

Seeking further evidence for the coordination of the Li^+ ions to the ether oxygen atoms of the POE chains at $n \leqslant 40$, we have considered the FT-Raman spectra of all the materials studied in the region where the polymer CH_2 groups absorb due to the rocking vibration mode (rCH$_2$) (Fig. 2). The so-called "oxygen breathing" mode [25] is detected in this range of wavenumbers. Fig. 2 reveals that the FT-Raman rCH$_2$ region of the doped hybrids with $n > 20$ closely resemble that of the non-doped matrix (not shown) [17]. The incorporation of more LiTFSI ($n = 20$) leads, however, to the growth of a new feature at approximately 865 cm^{-1}, which becomes the dominant event in

[1] PeakFit is a product of Jandel Corporation, 2591 Rerner Boulevard, San Rafael, CA 94901, USA.

the case of the more concentrated samples with $n = 8$ and 5 (Fig. 2). This feature is correlated with the process of POE chain wrapping around the Li^+ ions and typically accompanies complexation [23,26,27] corresponding to the establishment of *gauche* conformations in the O–C–C–O segments [26].

Thus the beginning of cation/ether oxygen bonding has been detected at $n = 40$ in the νCOC region and at $n = 20$ in the rCH_2 region. We will discuss again this particular issue below.

3.2. Cation/cross-link interaction

The examination of the FT-IR spectra of the d-U(2000)$_n$ LiTFSI hybrids in the "amide I" region (1850–1600 cm^{-1}) allows us to determine the ranges of salt concentration in which the carbonyl oxygen atoms of the urea cross-links bond to the Li^+ ions. This analysis enables us to obtain in parallel valuable information concerning the extent of hydrogen bonding in these xerogels.

The FT-IR spectra of representative d-U(2000)$_n$LiTFSI xerogels in the "amide I" region are reproduced in Fig. 3. The results of the curve-fitting performed in this band envelope with representative samples and the composition dependence of the area of the resolved components are illustrated in Fig. 4a and b, respectively. The frequency of the individual components of the "amide I" region and their assignment are listed in Table 1.

The "amide I" region of the di-ureasils corresponds to the amide I [28] region of polyamides [29]. The amide I mode, essentially due to the C=O stretching vibration, is sensitive to the specificity and magnitude of hydrogen bonding [29]. Typically the amide I band consists of several components associated with different C=O environments in aggregates, associations or structures. As the absorption coefficients of C=O groups belonging to these various aggregates can be different, it is not possible to compare concentrations of different components. Only the changes suffered by each mode and detected as alterations of the integral area represent concentration variations of each aggregate [29,30].

Fig. 4a demonstrates that the addition of Li^+ ions to d-U(2000) affects the "amide I" profile over the entire range of compositions examined, a situation already reported for the triflate [17] and perchlorate [18]-based analogues. This interaction has dramatic consequences at $n \leqslant 20$ (Fig. 4a). The "amide I" band of the d-U(2000)$_n$LiTFSI samples with $n > 8$ was decomposed into five components located at 1750, 1720, 1683, 1662 and 1640 cm^{-1} (Fig. 4a and Table 1). At $n = 8$ a new component emerges at 1617 cm^{-1} (Fig. 4a and Table 1). At $n = 5$ the 1750 cm^{-1} peak vanishes (Fig. 4a and Table 1).

The 1750 cm^{-1} band is associated with the absorption of urea groups in which the N–H or C=O groups are "free" (F) [31]. The events at 1720, 1683 and 1662 cm^{-1} are assigned to the absorption of hydrogen-bonded C=O groups of disordered hydrogen-bonded POE/urea associations of increasing strength (D1, D2 and D3, respectively) [17,31] The 1640 and 1616 cm^{-1} features are ascribed to the absorption of C=O groups belonging to significantly more ordered hydrogen-bonded urea/urea associations, of increasing strength (O1 and O2, respectively) [17,31].

The graph illustrated in Fig. 4b provides better insight into the modifications that the hydrogen-bonded aggregates of the d-U(2000) hybrid undergo as the LiTFSI concentration is increased:

(a) In the most dilute xerogel examined ($n = 200$) the modifications detected are very subtle (Fig. 4b). The main changes worth noting are a slight increase of the fraction of species F, a reduction in the proportion of aggregates D1, D2 and D3, while in parallel the fraction of aggregates O1 rises.
(b) At $n = 40$ the fraction of F groups and that of the aggregates O1 suffers a decrease (abrupt and moderate, respectively). In contrast, the proportion of aggregates D1 and D2 increases slightly and the amount of aggregates D3 rises significantly.
(c) The further incorporation of guest salt ($n = 20$) results in a drastic reduction of the fraction of groups F and aggregates D1. Concomitantly more aggregates D2, D3 and O1 are formed.
(d) In d-U(2000)$_8$LiTFSI the proportion of the components D2, D3 and O1 continues to decrease moderately, the content of aggregates D1 suffers an increase and the amount of groups F remains practically constant (Fig. 4b). The formation of new hydrogen-bonded aggregates O2, stronger than the O1 aggregates, is also observed.
(e) In the most concentrated xerogel analysed ($n = 5$) the aggregates D1 practically disappear and all the urea groups become saturated (i.e. no carbonyl groups are left "free"). Simultaneously, the fraction of aggregates D2 and D3 decreases slightly, whereas that of the O1 and O2 aggregates increases markedly.

The massive destruction of d-U(2000) structures D1 at $n \leqslant 20$ is consistent with the fact that within this range of salt content the POE segments are intensely involved in the complexation of the Li^+ ions and as a consequence they can no longer interact to the same extent with the N–H groups of the urea linkages through hydrogen bonding.

3.3. Cation/anion interactions

3.3.1. Raman $\delta_s CF_3/\nu_s$ SNS region

The Raman $\delta_s CF_3$ band of the "free" imide ion appears at about 739 cm^{-1} [19]. This ion-pairing sensitive band shifts to higher wavenumbers upon coordination to the cation. We must note, however, that the assignment of this band has been a matter of intense of discussion. Bakker et al. [32] have reported that it has a marked νS–N character and therefore many authors prefer to associate it predominantly to the symmetric stretching mode of the SNS group (ν_aSNS) [33,34].

Fig. 5a and b show the results of the curve-fitting carried out in the FT-Raman $\delta_s CF_3/\nu_s$SNS region of selected LiTFSI-doped di-ureasil samples and the composition dependence of the area of the resolved components, respectively. The frequencies of the isolated components of this region and their assignments are listed in Table 1.

The FT-Raman $\delta_s CF_3/\nu_s$SNS region of the d-U(2000)$_n$LiTFSI with $n \geqslant 40$ was decomposed into a single component at 739 cm^{-1} (Fig. 5b and Table 1) associated with "free" TFSI ions [19,33,34]. At $n = 20$ the FT-Raman $\delta_s CF_3/\nu_s$ SNS envelope was decomposed into two peaks situated at 743 and 739 cm^{-1} (Fig. 5 and Table 1). The former component, the intensity of which increases with salt concentration (Fig. 5a), is tentatively ascribed to the formation of contact ion pairs [19,33,34]. The occurrence of contact ion pairs at $n \leqslant 20$ correlates well with the data retrieved from the rCH_2 region that place the beginning of Li^+-POE complexation at $n = 20$. Fig. 5b demonstrates that

the concentration of "free" anions and that of the coordinated anions remains essentially the same at $40 < n \leqslant 8$. As expected, the fraction of "free" anions decreases significantly at the highest concentration analysed (i.e. $n = 5$), and, as a consequence, the proportion of associated species increases.

3.3.2. Infrared ν_aSNS/νCS, $\delta_a CF_3$ and $\delta_s CF_3/\nu_s$ SNS regions

In the 800–700 cm^{-1} interval of the FT-IR spectrum of the $TFSI^-$ ion three vibration bands are typically observed: the asymmetric stretching mode of the SNS group (ν_aSNS), the asymmetric deformation mode of the CF_3 group ($\delta_a CF_3$) and the $\delta_s CF_3/\nu_s$SNS mode.

The FT-IR spectra of the d-U(2000)$_n$LiTFSI hybrids with $n \geqslant 20$ in the νCS/ν_aSNS, $\delta_a CF_3$ and $\delta_s CF_3/\nu_s$SNS regions are depicted in Fig. 6. The results of the curve-fitting performed in the νCS/ν_aSNS and $\delta_s CF_3/\nu_s$SNS envelopes of selected samples are shown in the left and right insets of Fig. 6, respectively. The frequencies of the individual components of these regions and their assignments are listed in Table 1.

The FT-IR spectra of the xerogels with $n \geqslant 20$ reproduced in Fig. 6 display two intense events at 787 and 739 cm^{-1} and a weak, ill-defined event at 762 cm^{-1}. Upon addition of more salt ($n < 20$) the 787 and 739 cm^{-1} bands shift to 789 and 741 cm^{-1}, respectively (Fig. 6).

The FT-IR ν_aSNS region [33,34] of the d-U(2000)$_n$LiTFSI samples with $40 \geqslant n \geqslant 8$ was decomposed into two components at 791 and 784 cm^{-1} (Table 1 and left inset of Fig. 6). We associate the ν_aSNS band at 784 cm^{-1} with the occurrence of "free" $TFSI^-$ ions. We note, however, that Rey et al. [19] assigned this event to a νCS mode and attributed the band situated at 1061 cm^{-1} to the ν_aSNS mode (Table 1). The feature seen at 791 cm^{-1} in the FT-IR spectra of the di-ureasils is tentatively attributed to the presence of contact ion pairs.

The FT-IR $\delta_s CF_3/\nu_s$SNS band of the LiTFSI-doped di-ureasils with $40 \geqslant n \geqslant 8$ was resolved into two components at 742 and 738 cm^{-1} (Table 1 and right inset of Fig. 6). The 738 cm^{-1} feature is due to "free" anions [19,33,34] whereas the 742 cm^{-1} band is correlated with the formation of contact ion pairs.

The main conclusion that may be derived from the study of the $TFSI^-$ characteristic modes of the di-ureasils is that, although the Li^+ ions interact extensively with the anions for compositions $n \leqslant 40$, this process leads exclusively to the occurrence of contact ion pairs. This situation contrasts markedly with the lithium triflate [15,17] and lithium perchlorate [16,18]-doped di-ureasil analogues in which the formation of higher aggregates was also detected, a clear indication of the significantly higher tendency for ionic association in the di-ureasil systems doped with lithium salts incorporating triflate and perchlorate anions".

Finally, we are led to suggest that the species responsible for the existence of a room temperature conductivity maximum at $n = 35$ (3.2×10^{-5} S cm^{-1} at room temperature [11]) are "free" anions.

4. Conclusions

FT-IR and FT-Raman spectroscopic analyses were carried out on a di-ureasil hybrid system doped with a wide concentration range of LiTFSI ($200 \geqslant n \geqslant 5$). The saturation of the C=O groups of the urea cross-links by the Li^+ ions is attained at $n = 5$. At $n \leqslant 8$ new hydrogen-bonded urea–urea aggregates, considerably stronger than those established in the parent hybrid matrix, emerge. Complexation of the Li^+ ions by the POE chains at $n \leqslant 20$ is accompanied by the formation of contact ion pairs. "Free" anions are expected to be the main charge carriers of the room temperature conductivity maxima of the d-U(2000)$_n$LiTFSI electrolyte system.

Acknowledgements

This work was supported by the Fundação para a Ciência e a Tecnologia (POCI/QUI/59856/2004, POCTI/SFA/3/686). S. C. Nunes and P. Barbosa acknowledge the Fundação para a Ciência e a Tecnologia for grants (SFRH/BD/22707/2005 and SFRH/BD/13559/2003, respectively). The authors would like to express their appreciation of the referee's comments. The review provided us with an opportunity to improve the quality of the final version of the paper.

References

[1] M. Armand, M.T. Duclot, J.M. Chabagno, in: Proceedings of the Second International Meeting on Solid State Electrolytes, St. Andrews, Scotland, Extended Abstract 6.5, 1978.
[2] M. Armand, W. Gorecki, R. Andréani, in: B. Scrosati (Ed.), Second International Symposium on Polymer Electrolytes, Elsevier Applied Science, New York, 1990, p. 91.
[3] W. Gorecki, M. Jeannin, E. Belorizki, C. Roux, M.J. Armand, Phys. Condens. Matter 7 (1995) 6823.
[4] A. Vallée, S. Besner, J. Prud'homme, J. Electrochim. Acta 37 (1992) 1623.
[5] M. Hernandez, L. Servant, J. Grodin, J.-C. Lassègues, Ionics 1 (1995) 454.
[6] S. Lascaud, M. Perrier, A. Valeé, S. Besner, J. Prud'homme, M. Armand, Macromolecules 27 (1994) 7469.
[7] F. Gray, Polymer Electrolytes, RSC Materials Monographs, The Royal Society of Chemistry, London, 1997.
[8] C.J. Brinker, G.W. Scherer, Sol–gel Science: The Physics and Chemistry of Sol–Gel Processing, Academic Press, San Diego CA, 1990.
[9] M. Armand, C. Poinsignon, J.-Y. Sanchez, V. de Zea Bermudez, US Patent 5,283,310, 1994.
[10] V. de Zea Bermudez, C. Poinsignon, M.B. Armand, J. Mater. Chem. 7 (9) (1997) 1677.
[11] P. Barbosa, M.M. Silva, M.J. Smith, A. Gonçalves, S.C. Nunes, V. de Zea Bermudez, unpublished work.
[12] A.C.S. Bezerra, E.L. de Sá, F.C. Nart, J. Phys. Chem 101 (1997) 6443.
[13] S.J. Yao, S.K. Wolfson Jun, B.K. Ahn, C.C. Liu, Nature 241 (1973) 471.
[14] M. Yuqing, C. Jianrong, W. Xiahua, Trends Biotechnol. 22 (2004) 227.
[15] S.C. Nunes, V. de Zea Bermudez, D. Ostrovskii, M.M. Silva, S. Barros, L.D. Carlos, J. Rocha, M.J. Smith, E. Morales, J. Electrochem. Soc 152 (2) (2005) A429.
[16] M.M. Silva, S.C. Nunes, P.C. Barbosa, V. de Zea Bermudez, D. Ostrovskii, M.J. Smith, Electrochim. Acta 52 (4) (2006) 1542.
[17] S.C. Nunes, V. de Zea Bermudez, D. Ostrovskii, L.D. Carlos, J. Molec. Struct 702 (1–3) (2004) 39.
[18] S.C Nunes, V. de Zea Bermudez, D. Ostrovskii, P.B. Tavares, P.C. Barbosa, M.M. Silva, M.J. Smith, Electrochim. Acta, in press, doi:10.1016/j.electacta.2007.04.061.
[19] I. Rey, P. Johansson, J. Lindgren, J.C. Lassègues, J. Grondin, L. Servant, J. Phys. Chem. A 102 (19) (1998) 3249.
[20] K. Machida, T. Miyazawa, Spectrochim. Acta 20 (1964) 1865.
[21] H. Matsuura, T. Miyazawa, J. Polym. Sci 7(A-2) (1969) 1735.
[22] Å. Wedsjö, J. Lindgren, C. Paluszkiewicz, Electrochim. Acta 37 (1992) 1689.
[23] B.L. Papke, M.A. Ratner, D.F. Shriver, J. Electrochem. Soc 129 (7) (1982) 1434.
[24] I. Rey, J.-C. Lassègues, J. Grondin, L. Servant, Electrochim. Acta 43 (10–11) (1998) 1505.
[25] H. Sato, Y. Kusumoto, Chem. Lett. 6 (1978) 635.
[26] H. Ericson, B. Mattson, L.M. Torrel, H. Rinne, F. Sundholm,

Electrochim. Acta 43 (10–11) (1998) 1401.
[27] A. Brodin, B. Mattson, K. Nilsson, L.M. Torrel, J. Hamara, Solid State Ionics 85 (1996) 111.
[28] T. Miyazawa, T. Shimanouchi, S.-I. Mizushima, J. Chem. Phys 24 (2) (1956) 408.
[29] D.J. Skrovanek, S.E. Howe, P.C. Painter, M.M. Coleman, Macromolecules 18 (1985) 1676.
[30] M.M. Coleman, K.H. Lee, D.J. Skrovanek, P.C. Painter, Macromolecules 19 (1986) 2149.
[31] V. Zea Bermudez, L.D. Carlos, L. Alcácer, Chem. Mater. 11 (3) (1999) 569.
[32] A. Bakker, S. Gejji, J. Lindgren, J.K. Hermansson, M.M. Probst, Polymer 36 (23) (1995) 4371.
[33] A. Ferry, M. Furlani, A. Franke, P. Jacobsson, B.-E. Mellander, J. Chem. Phys. 109 (7) (1998) 2921.
[34] M. Furlani, A. Ferry, A. Franke, P. Jacobsson, B.-E. Mellander, Solid State Ionics 113–115 (1998) 129.

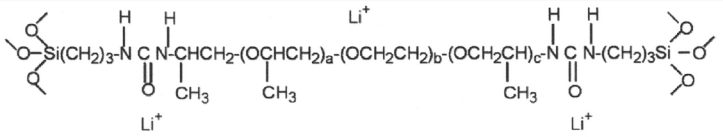

Scheme 1. Structure of the d-U(2000)$_n$LiN(SO_2CF_3)$_2$ di-ureasils.

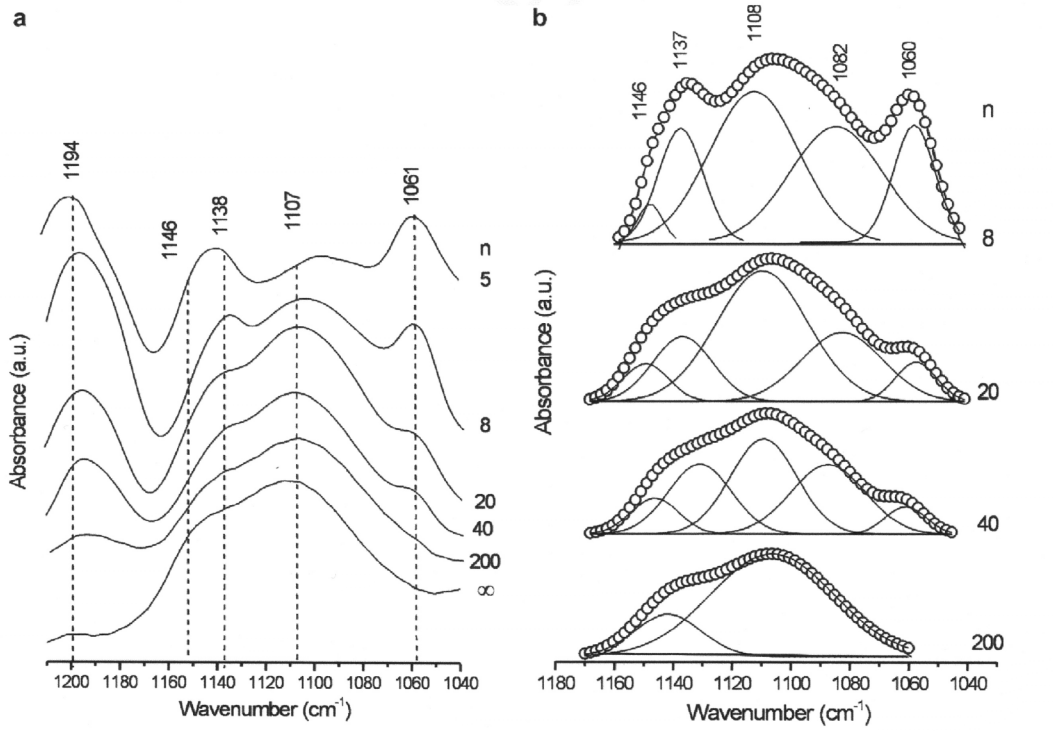

Fig. 1. FT-IR spectra in the 1210–1040 cm^{-1} interval region (νCOC, rCH$_2$, ν_sCF$_3$, ν_aSNS and ν_sSO$_2$ modes) (a) and curve-fitting in the 1180–1040 cm^{-1} interval region (b) of the selected d-U(2000)$_n$LiTFSI di-ureasils.

Table 1
Characteristic FT-IR and/or FT-Raman bands of the polymer and $TFSI^-$ ions in the spectra of the d-U(2000)$_n$LiTFSI di-ureasils

d-U(2000)$_n$ LiTFSI											
n										Attribution	Ref.
200		40		20		8		5			
IR	R	IR	R	IR	R	IR	R	IR	R		
1747	–	1749	–	1749	–	1750	–	–	–	"Free" N–H or C=O groups	[31]
1718	–	–	–	1722	–	1720	–	1719	–	Disordered hydrogen-bonded POE/urea associations	[17,31]
1685	–	–	–	1683	–	1685	–	1683	–		
1662	–	–	–	1662	–	1662	–	1663	–		
1640	–	–	–	1641	–	1640	–	1640	–	Ordered hydrogen-bonded urea/urea associations	[17,31]
–	–	–	–	–	–	1617	–	1616	–		
–	–	1194	–	1194	–	1194	–	1194		ν_aCF$_3$	[19,24]
1146	–	1146	–	1149		1147	–	1146	–	νCOC + rCH$_2$	[20–22]
–	–	1137	–	1137		1137	–	1137	–	$\nu_s^{o,p}$SO$_2$	[19,24]
1108	–	1108	–	1109		1112	–	1108	–	νCOC non-complexed	[20–22]
–	–	1082	–	1082		1083	–	1082	–	νCOC complexed	[23]
–	–	1060	–	1059		1059	–	1060	–	ν_aSNS	[19,24]
–	–	790	–	791	–	791	–	–	–	νCS/ν_aSNS Contact ion pairs	
–	–	784	–	784	–	784	–	–	–	"free" anions	[19]/[33,34]
–	–	762	–	761	–	761	–	761	–	ν_s(SNS)	[19]
–	–	741	–	740	743	742	741	–	742	δ_sCF$_3$/ν_sSNS Contact ion pairs	[33,34]
–	739	738	739	737	739	738	739	–	739	"free" anions	[19]/[33,34]

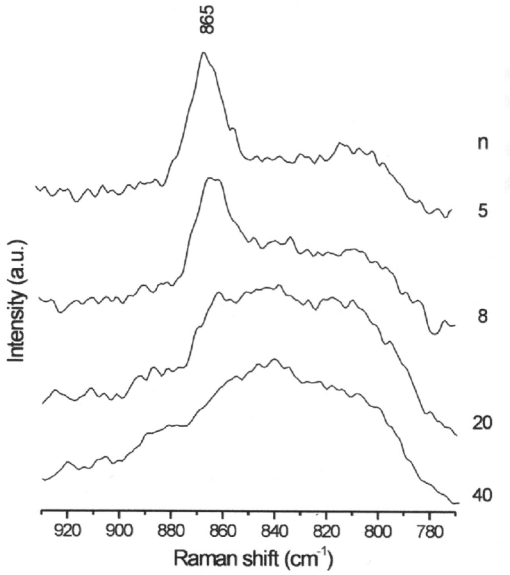

Fig. 2. FT-Raman spectra of selected d-U(2000)$_n$LiTFSI di-ureasils in the 925–775 cm^{-1} region.

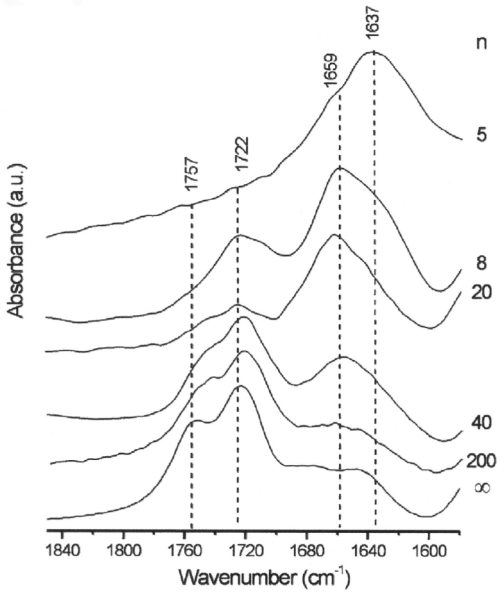

Fig. 3. FT-IR spectra of selected d-U(2000)$_n$LiTFSI di-ureasils in the "amide I" region.

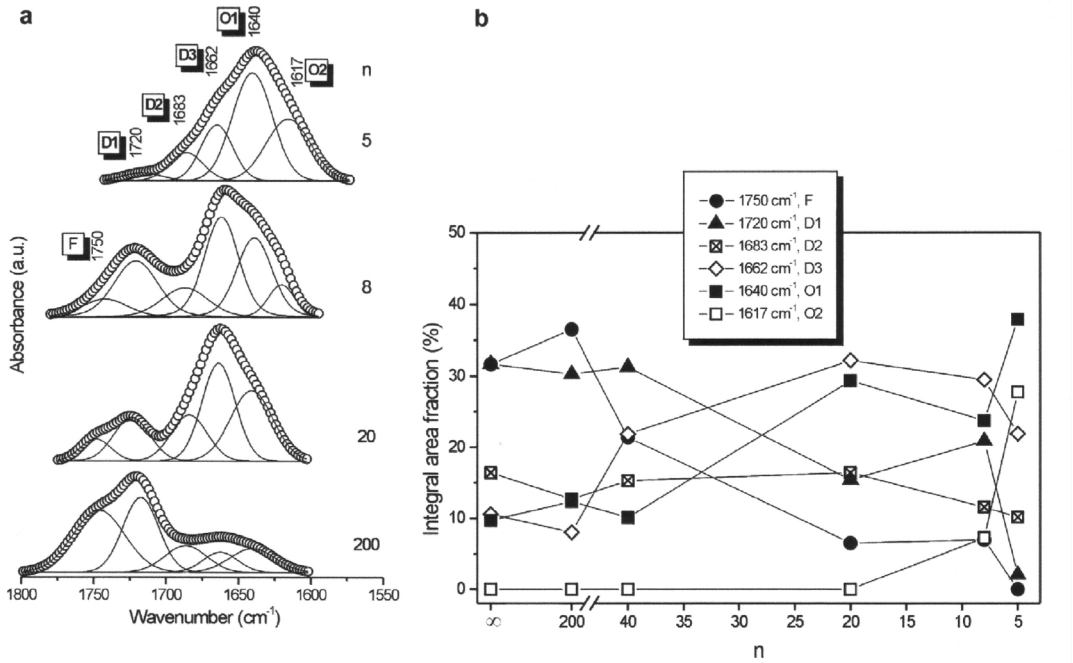

Fig. 4. Curve-fitting results of the "amide I" region of the d-U(2000)$_n$LiTFSI di-ureasils (a) and salt concentration dependence of the integral intensity of the different spectral resolved components (b).

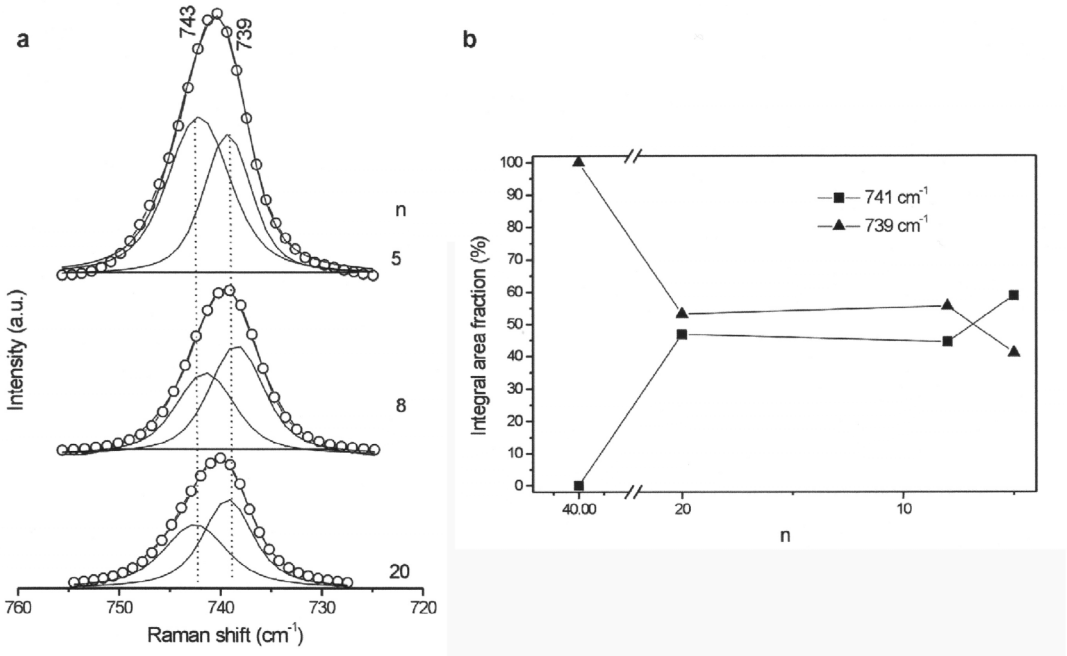

Fig. 5. Curve-fitting results of the FT-Raman $\delta_s CF_3/\nu_s SNS$ region of selected d-U(2000)$_n$LiTFSI di-ureasils. (a) and salt concentration dependence of the integral intensity of the different spectral resolved components (b).

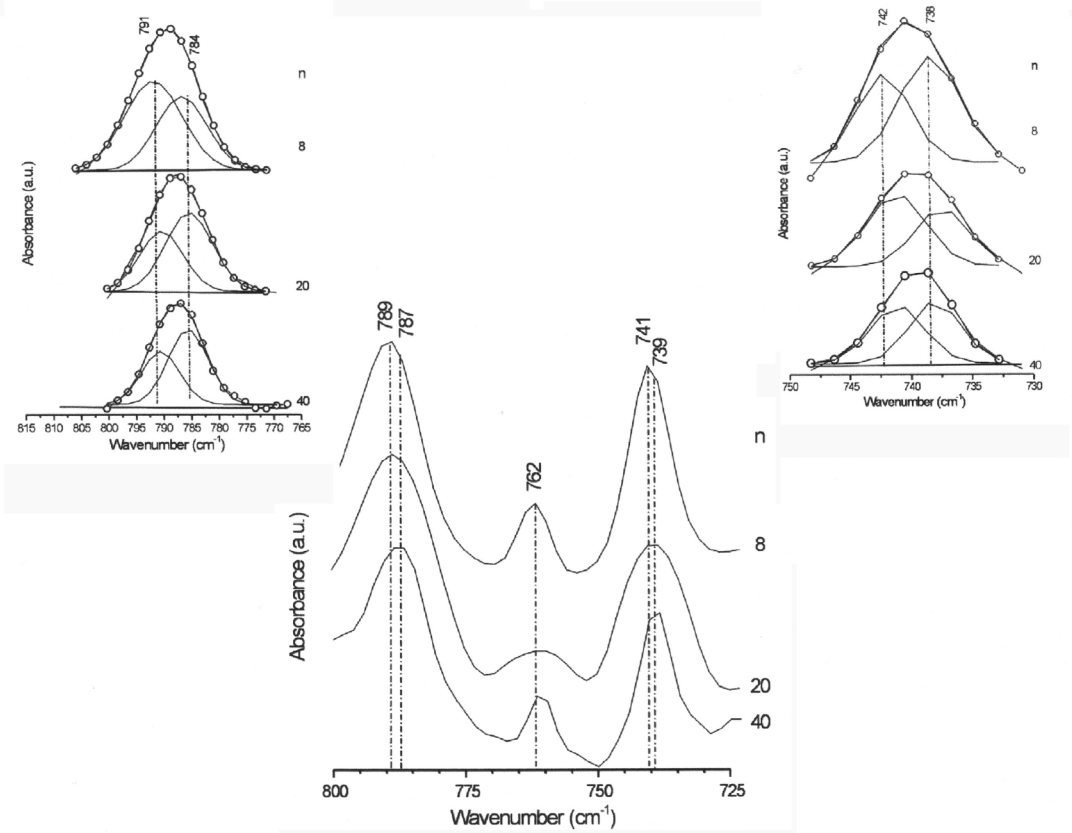

Fig. 6. FT-IR spectra of selected d-U(2000)$_n$LiTFSI of di-ureasils in the 800–700 cm^{-1} interval. Insets: results of the curve-fitting of the νCS/ν_aSNS (left) and $\delta_s CF_3/\nu_s SNS$ (right) bands of selected doped samples.